Statistical properties of Er/Yb co-doped random Rayleigh feedback fiber laser

Han Wu (吴 函)[1*], Bing Han (韩 冰)[2], Zinan Wang (王子南)[2], and Houkun Liang (梁厚昆)[1**]

[1] College of Electronics and Information Engineering, Sichuan University, Chengdu 610064, China

[2] Fiber Optics Research Centre, School of Information and Communication Engineering, University of Electronic Science and Technology of China, Chengdu 611731, China

*Corresponding author: hanwu@scu.edu.cn

**Corresponding author: hkliang@scu.edu.cn

In this Letter, we experimentally investigate fast temporal intensity dynamics and statistical properties of the cladding-pumped Er/Yb co-doped random Rayleigh feedback fiber laser (EYRFL) for the first time, to the best of our knowledge. By using the optical spectral filtering method, strong and fast intensity fluctuations with the generation of extreme events are revealed at the output of EYRFL. The statistics of the intensity fluctuations strongly depends on the wavelength of the filtered radiation, and the intensity probability density function (PDF) with a heavy tail is observed in the far wings of the spectrum. We also find that the PDF of the intensity in the central part of the spectrum deviates from the exponential distribution and has the dependence on the laser operating regimes, which indicates some correlations among different frequency components exist in the EYRFL radiation and may play an important role in the random lasing spectrum stabilization process.

1. Introduction

The random fiber laser operating via Rayleigh scattering was first demonstrated in 2010 in a standard telecommunication fiber span, which provides both the randomly distributed Rayleigh feedback and the Raman gain[1,2]. With the intrinsic cavity-free configuration and "modeless" spectrum, random Raman fiber lasers (RRFLs) have unique properties and advantages such as high efficiency/high output power[3], ultra-broad wavelength tunability[4–6], and flat-amplitude multi-wavelength operation[7,8]. A number of important applications of RRFL have been explored, such as remote sensing[9], speckle-free imaging[10], and supercontinuum generation[11,12]. Apart from the studies on improving the performance and pursuing its applications, RRFL has also triggered extensive investigations on its fundamental physical properties. Models based on the wave kinetic theory[13] and the nonlinear Schrodinger equation[14] are developed to describe the spectral and temporal properties of RRFL. Experimental measurements of spectral and temporal properties of RRFL have also been carried out very recently. In the spectral domain, a scanning Fabry–Perot interferometer was used to realize the real-time spectrum measurement of RRFL, and narrow spectral components with temporally varying

intensity were revealed for the first time[15], to the best of our knowledge. The Lévy spectral intensity statistics was further presented in RRFL[16], and the statistical evolution with the pump power was found similar to the case of higher-dimensional random lasers[17] and random grating-based random fiber lasers[18]. In the temporal domain, Gorbunov and collaborators for the first time, to the best of our knowledge, experimentally investigated the temporal intensity dynamics of RRFL and discovered strong intensity fluctuations on a short time scale[19]. Through further use of the optical filtering method, accurate intensity statistics has been measured for separate spectral lines in multi-wavelength RRFL[20] and different spectral components of RRFL[21]. Besides, the optical rogue wave phenomenon was reported in incoherently pumped RRFL when the pump power was around threshold with the bandwidth-limited measurement[22].

On the other hand, the concept of random fiber lasers can be extended to various gain media, including the rare-earth (RE)-doped gain[23–25], Brillouin gain[26], and semiconductor amplification[27]. RE-doped random fiber lasers can be constructed by combining the RE-doped active fiber and passive single-mode fiber (SMF), which provide the gain and the randomly distributed feedback, respectively[23–25]. RE-doped randomly fiber

lasers can generate random lasing in different wavelength regions and have been used in several applications, such as the seed laser in a master oscillator power amplifier (MOPA) system[28,29], the pump source for a cascaded Raman fiber laser[30], supercontinuum generation[31], frequency conversion[32], and temporal ghost imaging[33]. In fact, the temporal dynamics property of RE-doped random fiber lasers is a crucial factor to determine the performance of the aforementioned applications, such as the spectral linewidth maintenance in MOPA[28,29], the spectral purity of the cascaded Raman lasing[6], and the spectral bandwidth and flatness of the supercontinuum source[31]. Compared to the conventional cavity-based RE-doped fiber laser, the RE-doped random Rayleigh feedback fiber laser has a much larger cavity length without stationary cavity modes. Therefore, as a new class of quasi-continuous wave (CW) laser sources, the study of temporal and statistical properties of an RE-doped random fiber laser with random Rayleigh scattering feedback is of both fundamental and practical interest and importance. Here, we present a detailed experimental investigation on the temporal dynamics on short time scale and statistical properties of erbium/ytterbium co-doped random Rayleigh feedback fiber laser (EYRFL) for the first time, to the best of our knowledge. The results reveal the different statistical properties for the different spectral components of radiation. It is also found that in the central part of EYRFL radiation, the statistical properties deviate from Gaussian and depend on the operating regimes of EYRFL, which indicates that some correlations among different frequency components exist in the EYRFL radiation.

2. Experimental Setup

The experimental setup to measure the temporal dynamics of EYRFL is shown schematically in Fig. 1. The 5-m-long double cladding erbium/ytterbium co-doped fiber (EYDF, Nufern EYDF-10 P/125-XP) is cladding pumped by a 976 nm multimode laser diode (LD) through a $(2 + 1) \times 1$ pump combiner, which provides the gain for the 1550 nm random lasing. A section of standard SMF with 5 km length is attached after the EYDF as the randomly distributed feedback through Rayleigh scattering along the fiber. A highly reflective fiber Bragg grating

(FBG) with 1550 nm center wavelength and 0.2 nm 3 dB bandwidth connects to the signal port of the combiner, acting as a point reflector to form a half-open cavity structure combined with the randomly distributed Rayleigh scattering in the SMF. Before detection, two stages of isolators are additionally used to avoid inevitable back-reflections that may influence the operation of random lasing. A tunable filter with tunable center wavelength around 1550 nm and 0.09 nm 3 dB bandwidth is used to choose the specified spectral component in the EYRFL radiation; thus, the optical bandwidth of the filtered radiation is about 11.2 GHz. The filtered radiation is detected by a photodetector (PD) with 20 GHz bandwidth (Conquer KG-PD-20-DC) and then recorded by a high speed oscilloscope (OSC, R&S RTP016) with 16 GHz bandwidth. In measurements, we carefully tune the optical power into the PD by using a variable optical attenuator to make sure there is no saturation and, at the same time, ensure that there is enough average power to avoid the influence of the background noise of the PD. For spectrum measurements, we use an optical spectrum analyzer (OSA) with 0.02 nm resolution.
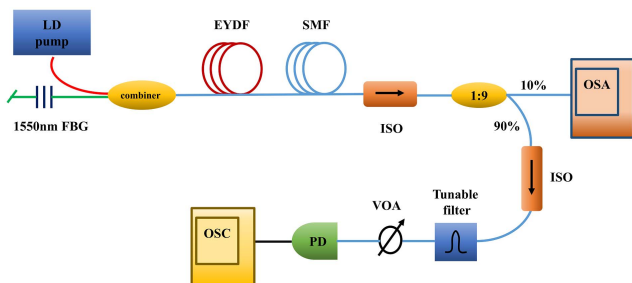
3. Experimental Results and Discussions

We first characterize the power and spectral performance of EYRFL, and the results are depicted in Fig. 2. The output power and the full spectrum of EYRFL before filtering are measured at the 90% and 10% ports of the coupler, respectively. Figure 2(a) shows the measured output power of the 1550 nm random lasing as a function of the launched pump power. The EYRFL has a threshold of 1.4 W, and the lasing power increases nearly
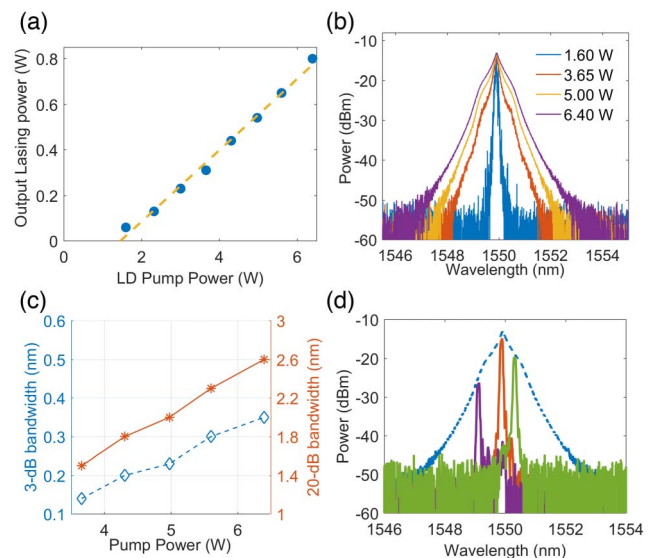
Fig. 2. Power and spectral properties of the EYRFL. (a) Output power versus pump power. (b) Output spectra at different pump powers. (c) Variation of −3 dB and −20 dB bandwidth of EYRFL with pump power. (d) Optical spectrum filtered by the narrow-bandwidth tunable filter. Dashed line: full spectrum of EYRFL; red line: in the central part; green line: detuned by 0.4 nm; purple line: detuned by 0.8 nm.

Fig. 1. Schematic of experimental setup. LD, laser diode; EYDF, erbium/ytterbium co-doped fiber; SMF, single-mode fiber; ISO, isolator; VOA, variable optical attenuator; PD, photodetector; OSC, oscilloscope; FBG, fiber Bragg grating; OSA, optical spectrum analyzer.

linearly with the slope efficiency of ∼16%. The efficiency could be enhanced by optimizing the length of EYDF and SMF. The spectral evolution with the increase of pump power is shown in Fig. 2(b). When the pump power of 1.6 W is just above the threshold, the lasing spectrum is unstable with the appearance of narrow spikes. The spectrum becomes stabilized and smooth when the pump power reaches 3.65 W. By further increasing the pump power, we can see the continuous broadening of the spectrum. Figure 2(c) records the variation of both −3 dB and −20 dB bandwidth of the spectrum. The −3 dB bandwidth is broadened from 0.14 nm to 0.35 nm, and the −20 dB bandwidth is broadened from 1.5 nm to 2.6 nm, as the pump power is increased from 3.65 W to 6.4 W. The understanding of such a spectrally broadening nature of EYRFL requires a reliable, full-bandwidth characterization of its temporal and statistical properties. Since the spectral bandwidth is several times larger than the electrical bandwidth of the OSC, we use the spectral filtering method to select narrow band spectral components at different spectral locations.

In our study, we choose three spectral components that are in the central part of the EYRFL emission spectrum, detuned by 0.4 nm and 0.8 nm from the central wavelength, respectively. The filtered spectra with three different central wavelengths are shown in Fig. 2(d). The −3 dB bandwidth of filtered spectrum is 0.09 nm (11.2 GHz) for all the three wavelengths, which is less than the bandwidth of the PD (20 GHz) and OSC (16 GHz), so there is no effect of frequency average, and we can measure the real intensities and accurate statistics at different spectral locations.

In order to make the statistical analysis, we record the long time traces containing 1.2×10^8 samples using the OSC at 40 GSamples/s sampling rate. The temporal dynamics and the measured intensity probability density function (PDF) of the filtered radiation at different spectral locations are plotted in Fig. 3. The pump power is fixed at 5 W. Strong fluctuations are observed in filtered radiations on sub-nanosecond time scale, as shown in Fig. 3(a). In the central part of the spectrum, we can record some extreme events with the intensity ∼6 times the average intensity. However, for the filtered radiation at the left edge of the spectrum detuned by 0.8 nm from the center, rare and intense events with peak powers that can be 30 times the average power can be observed. The PDFs of the filtered radiations intensity $I(t)$ normalized to its mean value $\langle I(t)\rangle$ have been computed from the experimental data and are plotted on a vertical logarithmic scale in Fig. 3(b). The black dashed line represents the exponential distribution PDF $(I_{\text{norm}}) = \exp(-I_{\text{norm}})$, in which $I_{\text{norm}} = I(t)/\langle I(t)\rangle$. For the radiation consisting of statistically independent frequency components with Gaussian statistics of the field, it must lead to the exponential intensity PDF[34−36]. However, for all of the filtered spectral components, the intensity PDF deviates from the exponential distribution. The intensity PDF of the radiation filtered in the wings of the spectrum is significantly non-exponential with the probability of extreme events much higher than that defined by the exponential distribution, and this phenomenon is similar to the situations in both conventional cavity-based Raman fiber
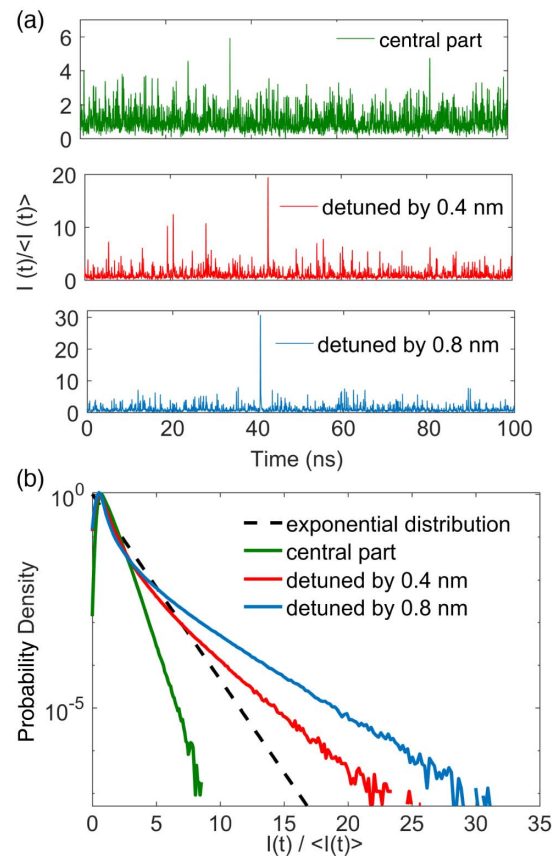

Fig. 3. (a) Temporal intensity dynamics and (b) intensity PDF of filtered random lasing radiations at different spectral locations. Green line: filtered in the central part; red line: detuned by 0.4 nm from the center; blue line: detuned by 0.8 nm from the center. The black dashed line in (b) represents the exponential distribution.

lasers[37,38] and RRFLs[21]. The probability of intense events becomes higher when the wavelength detuning from the spectral center is larger. Since the bandwidth of the point reflector at one fiber end is only 0.2 nm, the far spectral wings are generated at one fiber pass only. These rare extreme events located in the far spectral wings are associated with turbulent four-wave mixing interactions between different frequency components[37−39], although there are no stationary cavity modes in EYRFL.

The case is different in the central part of spectrum of EYRFL, where the non-exponential PDF with the high values of intensity is less probable than those governed by the exponential distribution that is observed. The spectral components in the central part of the spectrum experience multiple passes between the point reflector and random Rayleigh mirrors in the long SMF. The non-exponential PDF indicates some correlations among different frequency components that exist in EYRFL, even in the central part of the spectrum. However, the intensity PDFs exhibit exponential-like statistics in the previous measurements for the filtered narrowband central part in both the cavity-based Raman fiber laser[37,38] and the RRFL[21] or the individual spectral lines of multi-wavelength RRFL[20]. The difference may arise from the relatively large ratio of the filtered optical bandwidth to
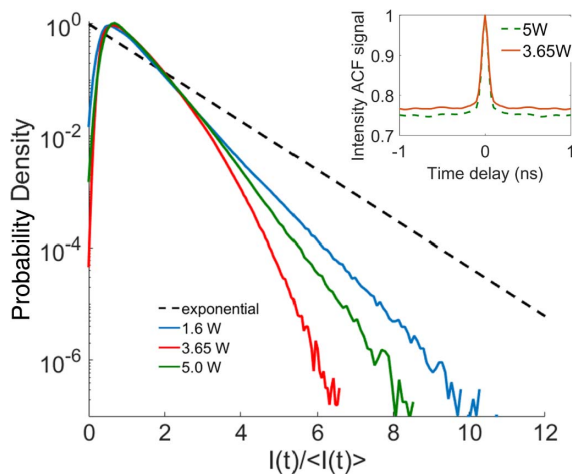
Fig. 4. Intensity PDFs of the filtered central part spectrum of EYRFL at different operating regimes. Insert: calculated intensity ACF of the filtered central part spectrum of EYRFL.

the total spectral bandwidth in our measurement. It should be noted that similar non-exponential intensity PDFs with significant decrease in probability at high intensity values have been found for the intra-cavity radiations with total spectral bandwidth of both cavity-based Raman fiber lasers[34,35] and RRFLs[14,19].

We then focus on the filtered central part of the spectrum and further study its statistical properties at different operating regimes. The intensity PDFs of the filtered central part spectrum of EYRFL at different operating regimes are also computed and shown in Fig. 4. It can be seen that the PDFs are all non-exponential and depend on the operating regimes of EYRFL. The PDF has the longest tail when the random laser is just above the threshold (1.6 W of pump power), and the spectrum is unstable. When the random lasing spectrum starts to be stable at 3.65 W pump power, there is significant decrease of probability to generate high intensities, which indicates that the correlations among different frequency components may play an important role in the random lasing spectrum stabilization process. However, the probability to generate high intensities increases when further increasing the pump power to 5 W. These results indicate the possible existence of different correlation behaviors among various frequency components of EYRFL radiation at different pump powers. We also calculate the intensity autocorrelation function (ACF) as $K(\tau) = \langle I(t)I(t+\tau)\rangle_t / \langle I(t)^2 \rangle_t$, as in the insert of Fig. 4. For completely Gaussian statistics, the ACF background level should be equal to 0.5[14,19,36]. The experimentally measured ACF background level of the filtered central part spectrum of EYRFL is around 0.75, which gives other evidence of existence of correlations in radiation.

4. Conclusions

In this Letter, we make the first, to the best of our knowledge, experimental investigation on the temporal intensity dynamics

and statistical properties of cladding-pumped EYRFL. With the narrowband tunable filter, we can make a reliable, full-bandwidth characterization of its temporal and statistical properties at different spectral locations. Strong fluctuations are observed in filtered radiations on the sub-nanosecond time scale with the experimental evidence of rare extreme events in EYRFL. The statistical properties highly depend on the spectral locations, and the intensity PDF with a heavy tail is observed in the far wings of the spectrum. We also experimentally find the non-exponential PDF with the high values of the intensity less probable than those governed by the exponential distribution in the central part of the spectrum. The shapes of non-exponential intensity PDFs of the central part spectrum also depend on the operating regimes of EYRFL when the pump power increases from 1.6 W to 5 W, indicating some correlations among different frequency components exist in the EYRFL radiation and may play an important role in the random lasing spectrum stabilization process.

References

1. S. K. Turitsyn, S. A. Babin, A. E. El-Taher, P. Harper, D. V. Churkin, S. I. Kablukov, J. D. Ania-Castañón, V. Karalekas, and E. V. Podivilov, "Random distributed feedback fibre laser," Nat. Photon. **4**, 231 (2010).
2. D. V. Churkin, S. Sugavanam, I. D. Vatnik, Z. Wang, E. Podivilov, S. A. Babin, Y. Rao, and S. K. Turitsyn, "Recent advances in fundamentals and applications of random fiber lasers," Adv. Opt. Photon. **7**, 516 (2015).
3. Z. N. Wang, H. Wu, M. Q. Fan, L. Zhang, Y. J. Rao, W. L. Zhang, and X. H. Jia, "High power random fiber laser with short cavity length: theoretical and experimental investigations," IEEE J. Sel. Top. Quantum Electron. **21**, 10 (2015).
4. L. Zhang, H. Jiang, X. Yang, W. Pan, S. Cui, and Y. Feng, "Nearly-octave wavelength tuning of a continuous wave fiber laser," Sci. Rep. **7**, 42611 (2017).
5. H. Wu, J. Song, J. Ye, J. Xu, H. Zhang, J. Leng, and P. Zhou, "Hundred-watt-level linearly polarized tunable Raman random fiber laser," Chin. Opt. Lett. **16**, 061402 (2018).
6. Y. Zhang, J. Song, J. Ye, J. Xu, T. Yao, and P. Zhou, "Tunable random Raman fiber laser at 1.7 μm region with high spectral purity," Opt. Express **27**, 28800 (2019).
7. S. Sugavanam, Z. Yan, V. Kamynin, A. S. Kurkov, L. Zhang, and D. V. Churkin, "Multiwavelength generation in a random distributed feedback fiber laser using an all fiber Lyot filter," Opt. Express **22**, 2839 (2014).
8. D. Leandro, S. Rota-Rodrigo, D. Ardanaz, and M. Lopez-Amo, "Narrow-linewidth multi-wavelength random distributed feedback laser," J. Lightwave Technol. **33**, 3591 (2015).
9. M. Fernandez-Vallejo, M. Bravo, and M. Lopez-Amo, "Ultra-long laser systems for remote fiber Bragg gratings arrays interrogation," IEEE Photon. Technol. Lett. **25**, 1362 (2013).
10. R. Ma, Y. J. Rao, W. L. Zhang, and B. Hu, "Multimode random fiber laser for speckle-free imaging," IEEE J. Sel. Top. Quantum Electron. **25**, 0900106 (2019).

11. R. Ma, Y. J. Rao, W. L. Zhang, X. Zeng, X. Dong, H. Wu, Z. N. Wang, and X. P. Zeng, "Backward supercontinuum generation excited by random lasing," IEEE J. Sel. Top. Quantum Electron. **24**, 0901105 (2018).

12. S. Arun, V. Choudhury, V. Balaswamy, R. Prakash, and V. R. Supradeepa, "High power, high efficiency, continuous-wave supercontinuum generation using standard telecom fibers," Opt. Express **26**, 7979 (2018).

13. D. V. Churkin, I. V. Kolokolov, E. V. Podivilov, I. D. Vatnik, M. A. Nikulin, S. S. Vergeles, I. S. Terekhov, V. V. Lebedev, G. Falkovich, S. A. Babin, and S. K. Turitsyn, "Wave kinetics of random fibre lasers," Nat. Commun. **6**, 6214 (2015).

14. S. V. Smirnov and D. V. Churkin, "Modeling of spectral and statistical properties of a random distributed feedback fiber laser," Opt. Express **21**, 21236 (2013).

15. S. Sugavanam, M. Sorokina, and D. V. Churkin, "Spectral correlations in a random distributed feedback fibre laser," Nat. Commun. **8**, 15514 (2017).

16. J. Li, H. Wu, Z. Wang, S. Lin, C. Lu, E. P. Raposo, A. S. L. Gomes, and Y. Rao, "Lévy spectral intensity statistics in a Raman random fiber laser," Opt. Lett. **44**, 2799 (2019).

17. J. Xia, J. He, K. Xie, X. Zhang, L. Hu, Y. Li, X. Chen, J. Ma, J. Wen, J. Chen, Q. Pan, J. Zhang, I. D. Vatnik, D. Churkin, and Z. Hu, "Replica symmetry breaking in FRET-assisted random laser based on electrospun polymer fiber," Annalen der Physik **531**, 1900066 (2019).

18. B. C. Lima, A. S. L. Gomes, P. I. R. Pincheira, A. L. Moura, M. Gagné, E. P. Raposo, C. B. de Araújo, and R. Kashyap, "Observation of Lévy statistics in one-dimensional erbium-based random fiber laser," J. Opt. Soc. Am. B **34**, 293 (2017).

19. O. A. Gorbunov, S. Sugavanam, and D. V. Churkin, "Intensity dynamics and statistical properties of random distributed feedback fiber laser," Opt. Lett. **40**, 1783 (2015).

20. O. A. Gorbunov, S. Sugavanam, I. D. Vatnik, and D. V. Churkin, "Statistical properties of radiation of multiwavelength random DFB fiber laser," Opt. Express **24**, 19417 (2016).

21. O. A. Gorbunov, S. Sugavanam, I. D. Vatnik, and D. V. Churkin, "Poisson distribution of extreme events in radiation of random distributed feedback fiber laser," Opt. Lett. **45**, 2375 (2020).

22. J. Xu, J. Wu, J. Ye, J. Song, B. Yao, H. Zhang, J. Leng, W. Zhang, P. Zhou, and Y. Rao, "Optical rogue wave in random fiber laser," Photon. Res. **8**, 1 (2020).

23. L. Wang, X. Dong, P. Shum, and H. Su, "Tunable erbium doped fiber laser based on random distributed feedback," IEEE Photon. J. **6**, 1501705 (2014).

24. Z. Hu, R. Ma, X. Zhang, Z. Sun, X. Liu, J. Liu, K. Xie, and L. Zhang, "Weak feedback assisted random fiber laser from 45°-tilted fiber Bragg grating," Opt. Express **27**, 3255 (2019).

25. Q. Meng, H. Wu, B. Han, J. Li, and Z. Wang, "LD-pumped random fiber laser based on erbium-ytterbium co-doped fiber," Photon. Sens. **10**, 181 (2020).

26. L. Zhang, C. Wang, Z. Li, Y. Xu, B. Saxena, S. Gao, L. Chen, and X. Bao, "High-efficiency Brillouin random fiber laser using all-polarization maintaining ring cavity," Opt. Express **25**, 11306 (2017).

27. H. Shawki, H. Kotb, and D. Khalil, "Modeling and characterization of a dual-wavelength SOA-based single longitudinal mode random fiber laser with tunable separation," OSA Continuum **2**, 358 (2019).

28. Z. Wang, P. Yan, Y. Huang, J. Tian, C. Cai, D. Li, Y. Yi, Q. Xiao, and M. Gong, "An efficient 4-kW level random fiber laser based on a tandem-pumping scheme," IEEE Photonics Technology Letters **31**, 817 (2019).

29. Y. Shang, M. Shen, P. Wang, X. Li, and X. Xu, "Amplified random fiber laser-pumped mid-infrared optical parametric oscillator," Chin. Opt. Lett. **14**, 121901 (2016).

30. H. Wu, Z. Wang, Q. He, W. Sun, and Y. Rao, "Common-cavity ytterbium/Raman random distributed feedback fiber laser," Laser Phys. Lett. **14**, 65101 (2017).

31. L. Chen, R. Song, C. Lei, W. Yang, and J. Hou, "Random fiber laser directly generates visible to near-infrared supercontinuum," Opt. Express **27**, 29781 (2019).

32. S. Rota-Rodrigo, B. Gouhier, C. Dixneuf, L. Antoni-Micollier, G. Guiraud, D. Leandro, M. Lopez-Amo, N. Traynor, and G. Santarelli, "Watt-level green random laser at 532 nm by SHG of a Yb-doped fiber laser," Opt. Lett. **43**, 4284 (2018).

33. H. Wu, B. Han, Z. Wang, G. Genty, G. Feng, and H. Liang, "Temporal ghost imaging with random fiber lasers," Opt. Express **28**, 9957 (2020).

34. D. V. Churkin, S. V. Smirnov, and E. V. Podivilov, "Statistical properties of partially coherent cw fiber lasers," Opt. Lett. **35**, 3288 (2010).

35. P. Walczak, S. Randoux, and P. Suret, "Statistics of a turbulent Raman fiber laser," Opt. Lett. **40**, 3101 (2015).

36. A. E. Bednyakova, O. A. Gorbunov, M. O. Politko, S. I. Kablukov, S. V. Smirnov, D. V. Churkin, M. P. Fedoruk, and S. A. Babin, "Generation dynamics of the narrowband Yb-doped fiber laser," Opt. Express **21**, 8177 (2013).

37. D. V. Churkin, O. A. Gorbunov, and S. V. Smirnov, "Extreme value statistics in Raman fiber lasers," Opt. Lett. **36**, 3617 (2011).

38. S. Randoux and P. Suret, "Experimental evidence of extreme value statistics in Raman fiber lasers," Opt. Lett. **37**, 500 (2012).

39. S. A. Babin, D. V. Churkin, A. E. Ismagulov, S. I. Kablukov, and E. V. Podivilov, "Four-wave-mixing-induced turbulent spectral broadening in a long Raman fiber laser," J. Opt. Soc. Am. B **24**, 1729 (2007).